Optimization of UV LED-Curable Ink for Reverse-Offset Roll-to-Plate (RO-R2P) Printing

Kayna Lee Mendoza, Ada Ortega & Nam Soo Kim

Journal of Electronic Materials

ISSN 0361-5235
Volume 44
Number 3

Journal of Elec Materi (2015) 44:784-791
DOI 10.1007/s11664-014-3506-6

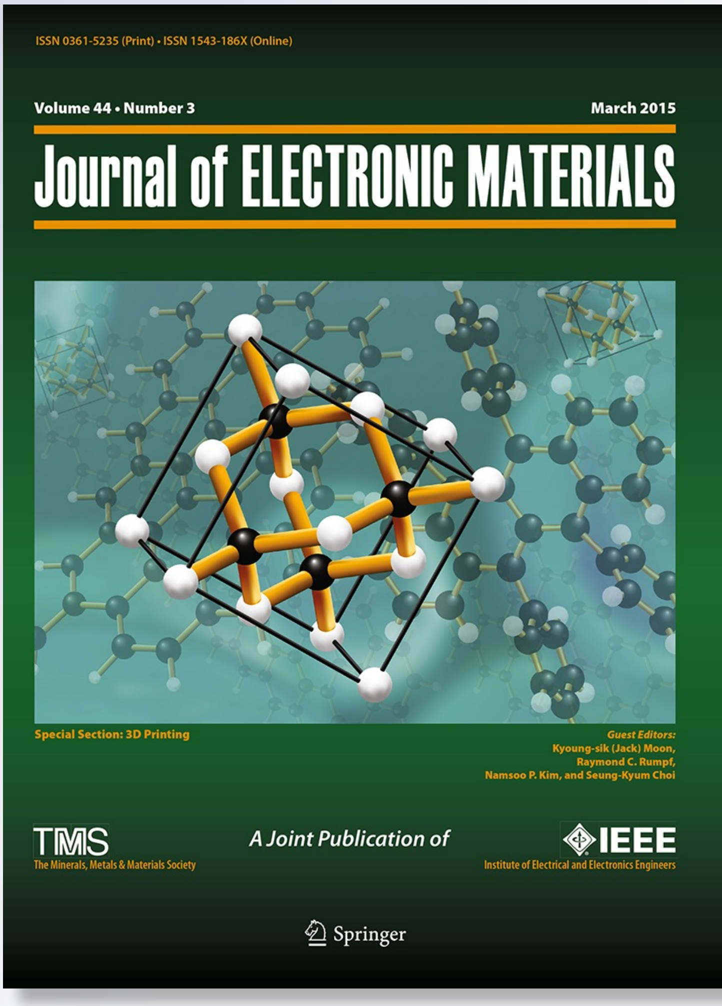

Springer

Journal of ELECTRONIC MATERIALS, Vol. 44, No. 3, 2015
DOI: 10.1007/s11664-014-3506-6

Optimization of UV LED-Curable Ink for Reverse-Offset Roll-to-Plate (RO-R2P) Printing

KAYNA LEE MENDOZA,[1,2] ADA ORTEGA,[1,3] and NAM SOO KIM[1,4]

1.—Department of Metallurgical and Materials Engineering, University of Texas at El Paso, 500 W. University Ave., El Paso, TX 79968-0520, USA. 2.— kaynalee.mendoza8@gmail.com. 3.— ajortega4@gmail.com. 4.—e-mail: nkim@utep.edu

Reverse-offset roll-to-plate printing has become increasingly popular in the printing industry because of the ease with which the printing process can be manipulated to achieve a high-resolution pattern with line widths as narrow as 5 μm with precision and accuracy. The printing procedure involves three stages, and a roller is required to transfer ink from each stage. The substrates used throughout this experiment were chosen by measuring their contact angles (θ) and using them in accordance with the sequence: θ (Stage 1) $> \theta$ (roller) $> \theta$ (Stage 2) and θ (Stage 3). An ultraviolet (UV) light-emitting diode (LED)-curable ink was used during the printing process; however, the pristine solution of this ink was unsuitable for printing a final pattern on the substrate because of its viscosity. Diluting the solution of the UV LED-curable ink with 40% CH_3OH resulted in reduced viscosity. The original solution had a viscosity of approximately 40.7 cP whereas that of the diluted solution was approximately 25 cP. The two solutions behaved as non-Newtonian, dilatant, shear-thickening fluids. The UV LED-curable ink solutions, both dilute and non-dilute, were successfully printed by use of an inkjet printer and three-dimensional printing methods.

Key words: Reverse-offset printing, roll to plate, RO-R2P, contact angle, viscosity, UV LED

INTRODUCTION

Electronic printing technology has become highly important because if its variety of applications in solar cells, and for radio-frequency identification tags and display technology.[1] The most common non-contact printing methods include gravure offset printing, flexographic printing, screen printing, and reverse-offset printing,[2–6] The precision and accuracy of each of these techniques, in terms of line width, line edge straightness, thickness, and thickness deviation, varies. Although many non-contact printing processes are capable of transferring high-quality images on to flexible substrates, reverse-offset can result in the highest-resolution printing of patterns with line widths as narrow as 5 μm, with small thickness deviations.[7] However, these specifications are only possible when ideal printing conditions are met.

The main factors affecting the quality of the reverse-offset printing are the rheological properties of the ink and its interfacial relationship with the substrates involved in the process.[8–10] In reverse-offset printing, the ink is coated on to an initial substrate and the roller must transfer the ink between several stages before the process is complete. When the roller has a continuous layer of ink it has to roll over a cliché containing the negative of the desired pattern. The interfacial energy between the cliché and the ink must be higher than that between the roller and the ink for the pattern to be formed. Therefore, the wetting properties of the ink

(Received May 30, 2014; accepted October 30, 2014; published online December 6, 2014)

on the substrate determine whether the ink is successfully transferred.

The smaller the contact angle between the droplet and the substrate, the more well spread the droplet; the larger the contact angle the more spherical-shaped the droplet, which does not allow the liquid to be uniformly spread.[11,12] A liquid vapor interfacial energy that has a smaller contact angle shows that the adhesive forces are stronger than the cohesive forces between the molecules, which allows the molecules to spread on the substrate rather than sticking to each other. In the reverse-offset printing process, the contact angle between stages and the roller must be optimized to aid the ink-transfer process.

Printing inks usually behave as non-Newtonian fluids, mainly because of their novel components and the interaction between these in the ink. This behavior presents a challenge in printing, because non-Newtonian fluids are defined by the ratio of shear stress (τ) to shear rate (γ). As the shear rate (γ) is varied, the viscosity of the fluid will change. In non-contact printing methods, for example reverse offset, the viscoelastic behavior becomes an important aspect of the ink-transfer process. Although numerous studies have characterized the effects of the viscoelastic properties of ink in non-contact printing, such studies have focused mainly on gravure offset or roll-to-plate.[4,13,14] Thorough research is needed on the printability of non-Newtonian fluids by reverse offset to further the development of the method. Figure 1 depicts the behavior of Newtonian and non-Newtonian fluids.

UV LED-curable ink has a variety of benefits, for example superior product quality, successful curing within seconds by use of UV radiation, weathering-resistant protective coating, safe handling of coating materials, and reduced cycle times, which increase production capacity and facilitate use of heat-sensitive substrates.[15] Because of the benefits of UV LED-curable ink, the printing industry has adopted this ink and its coating procedures, because they emit little or no volatile organic compounds (VOC), e.g. solvents, they do not dry during the printing process, and the curing equipment occupies much less space than conventional thermal drying conveyors.[16] Research has revealed that UV LED-curable ink as a coating protects against extreme temperatures and weather conditions; the materials themselves are environmental friendly, resistant to mechanical impact, low cost, and have the desired optical characteristics. Crosslinking of new particles in the solutions has led to the development of new polymer ink compositions for printed coatings on packaging with enhanced and durable barrier performance and other improved characteristics, for example desired mechanical strength and optical properties, believed to be of benefit for different packaging applications.[17]

In this study the rheological and wetting properties of a UV-curable ink were characterized to determine its suitability for reverse-offset printing. UV-curable ink was selected because, in comparison with other inks used for printing, for example flexographic ink, the market is expected to grow at 3% per annum, and the market for UV LED-curable ink is growing at 17% per annum.[16] A new approach to predicting the printability of an ink by reverse offset has been tested for a variety of substrates. It was concluded that even if contact angle requirements are met, the viscoelastic behavior of the ink is also extremely important to the accuracy of patterns.

EXPERIMENTAL

Viscosity Measurement

Viscosity was measured by use of a Brookfield LVDV-I Prime viscometer with an SC4-DIN-82 spindle. A liquid of known viscosity (60 cP, 9 mL) was used to check machine accuracy and precision. With the viscometer used at a speed of 6.283 radians per second, the viscosity read 58.6 cP. For measurement of the unknown viscosity of pristine UV LED-curable ink, 9 mL was used. When the viscometer was used at a speed of 5.236 radians per second the viscosity reading was 40.7 cP. When the pristine UV LED-curable ink was diluted with 40%

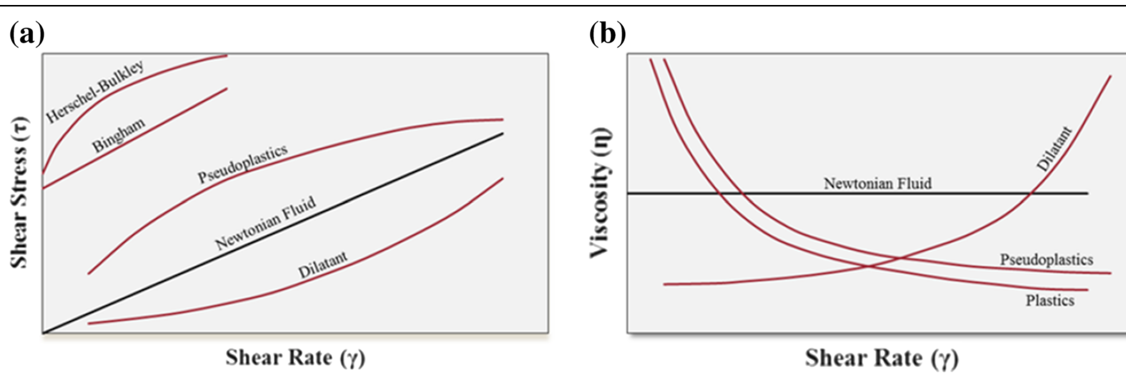

Fig. 1. Graphs of the behavior of Newtonian and non-Newtonian fluids: (a) shear stress as a function of shear rate; (b) viscosity as a function of shear rate.

methanol the viscosity was 25 cP at a speed of 5.236 radians per second.

Contact Angle Measurement

The contact angle between the UV LED-curable ink in the two solutions and nine different materials (M1, M2, M3, M4, M8, glass cliché, PET, kapton PV 9101 (polyimide, DuPont), kapton PV 9102 (polyimide, DuPont)) was measured by use of a Rame-Hart model 250 Std G/T goniometer with DROPimage Advanced software. The contact angle was measured by use of the drop method, by use of a micro syringe; reported results for the contact angle are mean values based from three replicate experiments. Each droplet of liquid was 10 μl.

Reverse-offset printing

A schematic diagram of the reverse-offset printing process is shown in Fig. 2. The system has one roller, and printing is performed using three stages: the off process, the patterning process, and the set process. In the coating process, the UV LED polymer ink is spin coated by use of an Alibaba model ACE-200 instrument: 18 s at 628.318 radians per second was used for the pristine solution and for 18 s at 104.720 radians per second for the diluted solution. This is followed by the off process, which transfers ink from Stage 1 to the roller. The roller is then coated with the UV LED polymer ink and transfers the ink on to the embossed parts of the cliché, leaving the negative of the desired pattern on the roller; this is the patterning process. The ink left on the roller is transferred to the final substrate in the set process. During this process, the pressure and speed are maintained at 0.10 N and approximately 2 cm/s, respectively.

Inks

In this study three types of UV LED-curable ink were used, each supplied by Chokwang Paint. Each UV LED-curable ink was an acrylate-based solution, which provides insight into its mechanical properties, because there are several groups of UV-curing polymers. The viscosity of the pristine UV LED-curable ink was approximately 40.7 cP and the viscosity of the UV ink diluted with 40% methanol was approximately 25 cP. The LED–UV liquid used was an acrylate oligomer containing hydroxycyclohexyl phenyl ketone polyethylene glycol 400-diacrylate and hydroxypropyl acrylate (Chokwang Paint)

Cliché

The cliché used for the second stage of the patterning process was made of glass and comprised four different patterns. In this experiment a glass cliché with varied pattern sizes ranging from 5 μm to 50 μm was used to test the printing process.

Substrates

The different substrates used in these were M1, M2, M3, M4, M8, glass cliché, PET, kapton PV 9101 (polyimide, DuPont), and kapton PV 9102 (polyimide, DuPont). These flexible, durable, and temperature-tolerant substrates have set the standard for long-term reliability and high performance in the electronics industry. By measuring the contact angle between the UV LED-curable ink (liquid) and the substrates (solid), Stage 1, Stage 2, Stage 3, and the roller can be determined for the reverse-offset roll-to-plate printing process.

RESULTS AND DISCUSSION

Viscosity

In this work the viscosities of the UV LED-curable inks were studied. The dilute solution and the pristine solution were used to determine the optimum viscosity for the roll to plate printing method. Analysis of the results from viscosity measurement showed the two UV inks behaved as dilatant non-Newtonian fluids. A dilatant (shear thickening) material is one for which the viscosity increases as shear rate increases; the properties of a material or fluid are determined by particle size, particle shape, and particle distribution. Although no particles were added, the pristine solution contains unknown additives. The UV LED-curable ink components are an acrylate oligomer, 1-hydroxycyclohexyl phenyl ketone polyethylene glycol 400-diacrylate and 2-hydroxypropyl acrylate additive. Because this additive is present in the pristine solution and the diluted solution, it caused dilatant behavior in the UV LED-curable ink. A dilatant fluid is also known as a shear thickening fluid (STF); this

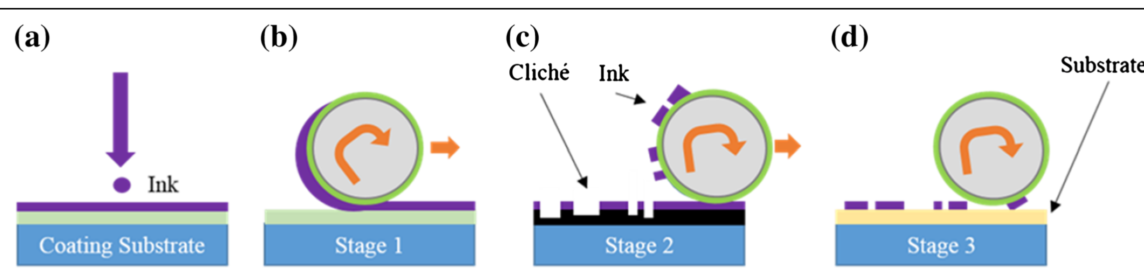

Fig. 2. Reverse-offset roll-to-plate printing: (a) coating process, (b) off process, (c) patterning process, and (d) set process.

behavior is dependent on interparticle forces and as long as the Van der Waals forces are dominant, the particles remain in layers acting like a fluid. However, once a shear force is applied, the particles are no longer in suspension but have agglomerated, behaving like a solid.

Figure 3 shows plots of shear stress as a function of shear rate for the two solutions. As shear rate increases, shear stress increases. Similar to Fig. 3, Fig. 4 shows a plot of viscosity as a function of shear rate for the two solutions. As shear rate increases, the viscosities of both the pristine and diluted solution increase.

Contact Angle

The R2P printing process was analyzed to determine the optimum relationship between contact angle and substrate at each stage of the printing process. Equation 1 was developed, in which selection of printing substrates and inks is standardized according to contact angle. To develop the optimum relationship in this experiment, the UV LED polymer ink was transferred from Stage 1 (the off process) to Stage 3 (the setting process) consecutively by use of the roller. Throughout this process, the roller removed the ink in Stage 1 and made direct contact in Stage 2 to transfer the UV LED-curable ink on to the cliché. The embossed parts of the cliché removed the ink from the roller but left the remaining ink with its patterns on the substrate of the roller. After this step, in Stage 3 the remaining UV LED polymer ink was transferred to the final substrate. From this information, the contact angles for the cliché and the final substrate should be smaller than that for the roller for optimum patterning quality while printing.

$$\theta\,(\text{Stage 1}) > \theta\,(\text{Roll}) > \theta\,(\text{Stage 2}),\ \theta\,(\text{Stage 3}) \quad (1)$$

Figure 5a shows results for contact angles between the pristine, 40.7 cP, and diluted solution, 25 cP, of the UV LED-curable ink and its different substrates. From this figure, M4 had the largest contact angle with the UV LED-curable ink ($\theta = 52.1°$) whereas PET had the lowest contact angle ($\theta = 20.5°$). According to Eq. 1, M4 substrate was used in the coating process and is set on Stage 1 for the off process. M8, M1, and M3 substrates are chosen for use on the roller which is the mechanism of transfer of the reverse-offset roll-to-plate printing process. The glass cliché is placed on Stage 2 where the patterning process occurs. M2, kapton PV 9101, kapton PV 9102, and PET substrates are all used on Stage 3 in the setting process, because of their their small contact angles. Similarly to the process used for choosing the optimal substrates for the pristine solution, the diluted solution, Fig. 5b shows the substrates with the highest potential for being used as the roller, Stage 1 and Stage 3, while Stage 2 remains constant. From this figure, the optimum substrates to be used for the roller are kapton PV 9102 and M8, according to Eq. 1. The substrates, kapton PV 9101 is most suitable for Stage 1 and PET is most suitable for Stage 3. Unlike Fig. 5a, the three substrates with the largest contact angles in Fig. 5b were not satisfactory for Stage 1 due to the solutions viscosity.

The plot in Fig. 6 shows the different contact angles for the three selected substrates used for the roller and the six other substrates used for Stage 1, Stage 2, and Stage 3, for the pristine UV LED-curable ink. Analysis of the information shows that the larger the contact angle difference between the substrate used for the roller and the substrates used for Stage 3, the more accurate and precise the printing pattern will be in reverse-offset roll-to-plate printing.

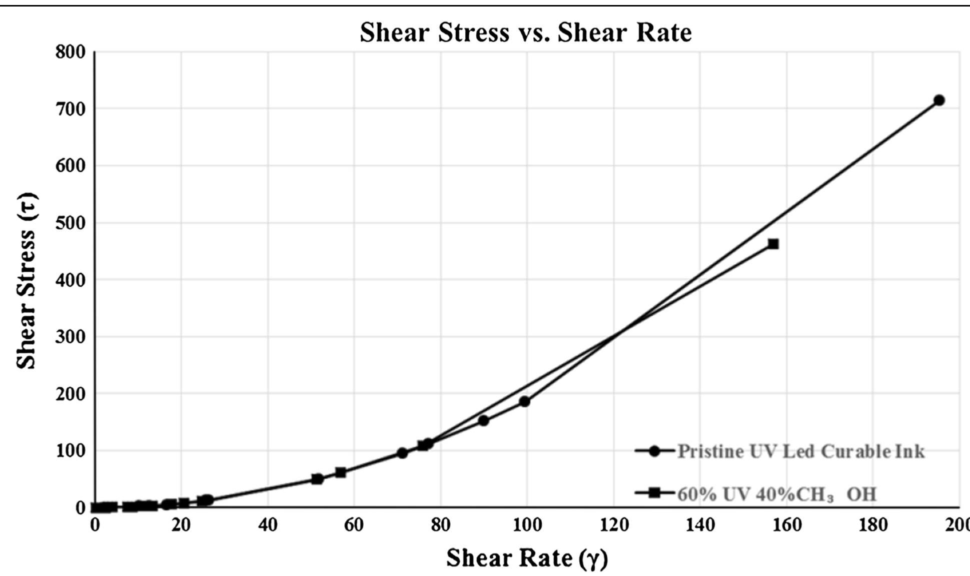

Fig. 3. Plot of shear stress as a function of shear rate for a dilatant non-Newtonian fluid.

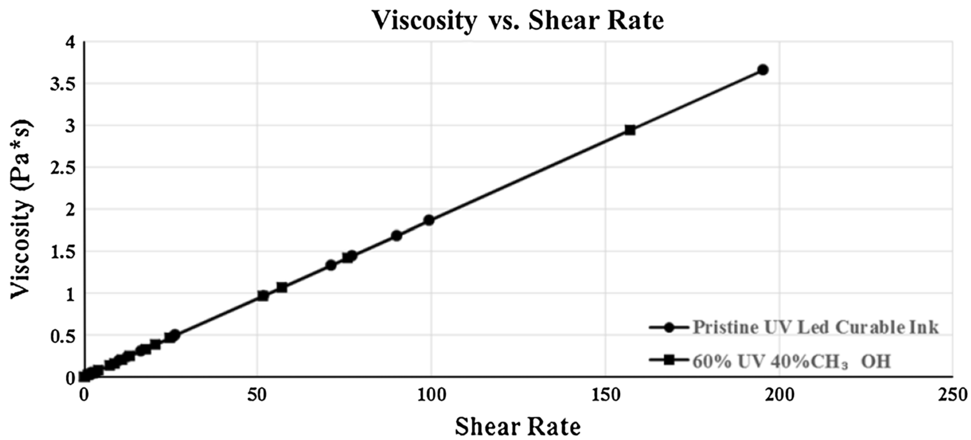

Fig. 4. Plot of viscosity as a function of shear rate for a dilatant non-Newtonian fluid.

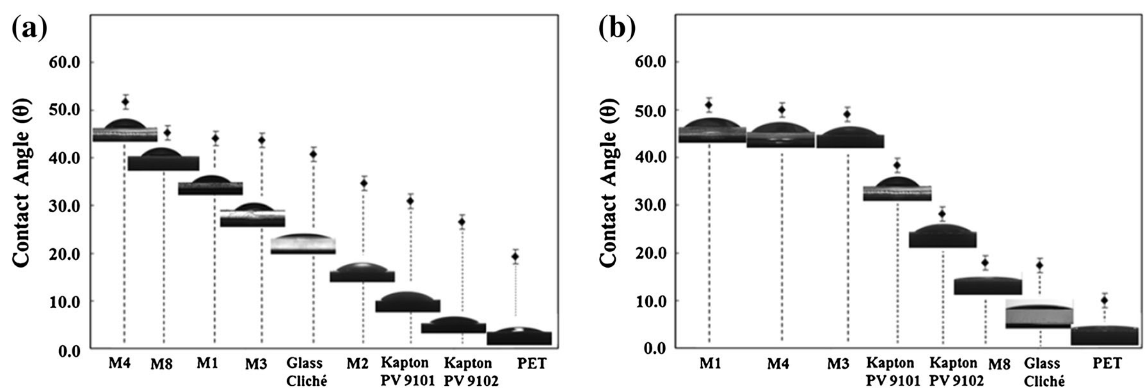

Fig. 5. (a) Images and results for contact angles between pristine UV LED-curable ink and nine different substrates; (b) images and data for contact angle between diluted UV LED-curable ink and eight different substrates.

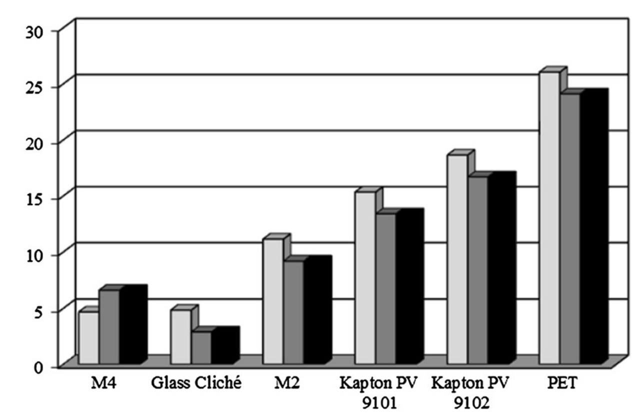

	M4	Glass Cliché	M2	Kapton PV 9101	Kapton PV 9102	PET
M8	4.67	4.84	11.14	15.34	18.64	26.04
M1	6.61	2.9	9.2	13.4	16.7	24.1
M3	6.61	2.9	9.2	13.4	16.7	24.1

Fig. 6. Graphical data for contact angle differences between the roller and Stage 1, Stage 2, and Stage 3 for the pristine solution.

The plot in Fig. 7 shows the different contact angles for the two selected substrates used for the roller and the substrates used for Stage 1 (kapton PV 9101), Stage 2 (glass cliché), and Stage 3 (PET) for the dilute solution of the UV LED-curable ink. Equation 1 indicates that the larger the contact angle difference for the roller and Stage 3, the more accurate and precise will be the pattern. At the beginning of the experiment, the contact angles were measured for eight possible substrates; however, as the ink was being spin coated at a speed 628.318 radians per second, it was not uniformly spread over the surface. Because of the wettability of the substrates by the UV LED-curable diluted ink solution, the spin coater was optimized and the speed reduced to 104.720 radians per second for 18 s. Testing the wettability for each substrates intended for Stage 1 and the roller showed the substrates M1, M4, and M3 were not suitable for the reverse-offset printing process because of the lack of uniform coating. The substrate with the next highest contact angle most suitable for Stage 1 was kapton PV 9101, because the diluted UV LED-curable ink solution was uniformly spread by spin coating at a speed of 104.720 radians per second for 18 s. This enabled successful transfer of ink from Stage 1 to the roller.

Figure 8 shows the patterns resulting from use of the different substrates (M8, M1, M3) were

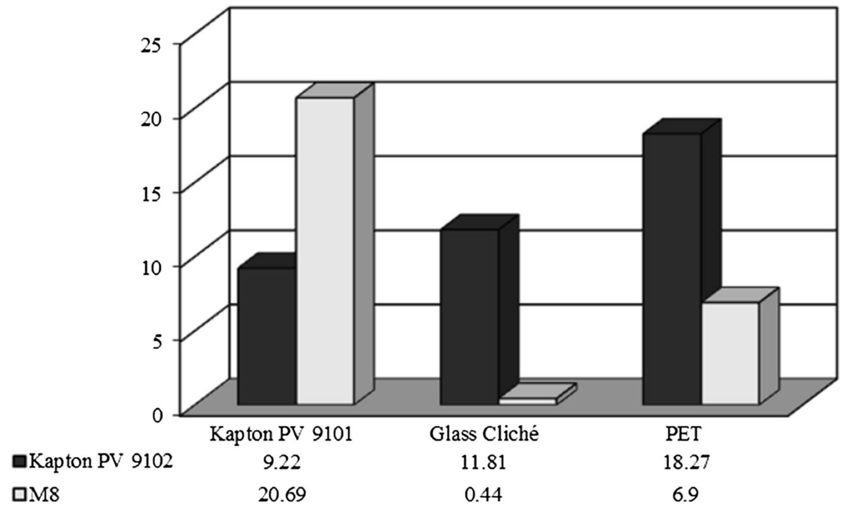

Fig. 7. Graphical data for contact angle differences between the roller and Stage 1, Stage 2, and Stage 3 for the diluted solution.

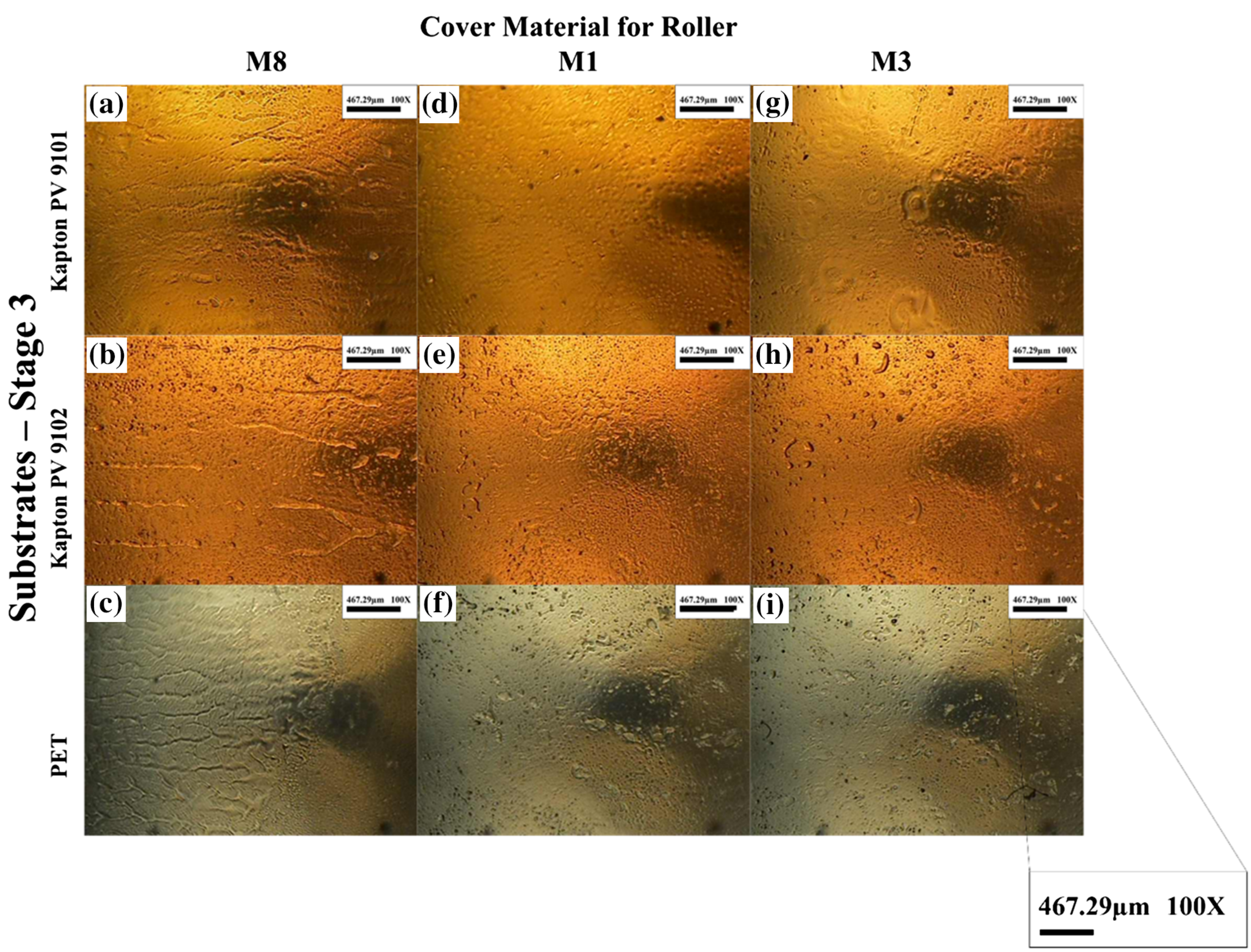

Fig. 8. Results from use of M8: (a) kapton PV 9101, (b) kapton PV 9102, (c) PET; use of M1: (d) kapton PV 9101, (e) kapton PV 9102, (f) PET; use of M3: (g) kapton PV 9101, (h) kapton PV 9102, (i) PET for roller in reverse-offset roll-to-plate printing (100× magnification).

used for the roller and for the final substrates (kapton PV 9101, kapton PV 9102, and PET), seen at 100× magnification by use of an optical microscope. In Fig. 8a–c the printed pattern is not visible. Although the method of using the contact angle to set up the reverse-offset print-

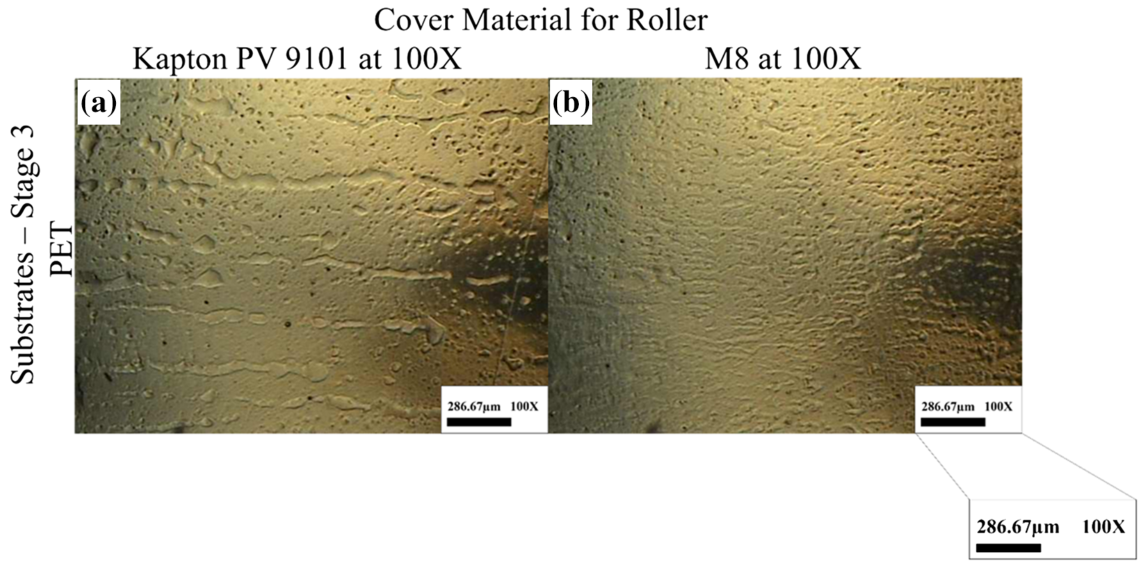

Fig. 9. Results from use of (a) kapton PV 9102 and PET, and (b) M8 and PET (100× magnification).

ing process was used, the substrates used in the setting process, off process, patterning process, and setting process were unsuitable for printing a high-quality pattern because of their similarity to the roller. In other words, the difference between the contact angles for M4 (Stage 1) and M8 (roller) was fairly small ($\Delta\theta = 4.67°$) so transfer of ink on to the roller was insufficient, therefore printing of high-quality patterns did not occur because of the lack of UV LED-curable ink on the substrate used for transferring the ink on to the cliché and from there to the final substrate.

Figure 8d–f shows the results for the printed pattern when M1 ($\theta = 44.6°$) was used for the roller. Similarly, when M8 was used as the roller, the final substrates were unable to produce a pattern on the cliché. The contact angle difference between M4 (Stage 1) and M1 (roller) is larger ($\Delta\theta = 6.61°$) than when M8 was used as the roller, meaning that transfer of UV LED-curable ink was easier, even though it is viscous in nature. During the patterning process (roller and the glass cliché), removal of a pattern was unsuccessful because of its viscous properties and the wettability of the two substrates. This resulted in a printed pattern inconsistent with the glass cliché.

Figure 8g–i shows the results for the printed pattern on the final substrate when M3 ($\theta = 44.6°$) was used as the roller. Although the contact angle was similar for M1 and M3, the wettability characteristics were different, resulting in a pattern on the final substrate. Because the contact angle difference is low ($\Delta\theta = 2.9°$), ink transferred from the roller to the glass cliché adhered much more easily, because of its physical properties. As the patterning process was occurring, transfer of ink from the roller to the embossed parts of the glass cliché was achieved and the remaining UV LED-curable ink remained on the roller. In this process, setting occurred and enabled the remaining ink on the roller to be transferred to the final substrate. The final patterns on the substrate were not continuous, because of the viscous nature of the ink, but a lightly lined pattern was achieved on each of the substrates.

Figure 9 shows the patterns resulting when different substrates (kapton PV 9102 and M8) were used for the roller and PET was used as the final substrate for Stage 3, measured at 100× magnification by use of an optical microscope. Figure 9a is the resulting pattern on the PET substrate when kapton PV 9102 was used for the roller. There are visible lines which are not continuous and do not reflect the pattern of the cliché. Figure 9b is the resulting pattern on the PET substrate when M8 was used for the roller. Similarly to the experiment with kapton PV 9102, the pattern created when M8 was the roller is insufficient.

CONCLUSION

Throughout the reverse-offset printing process, transfer of ink from the coating process to the final setting process is vital. This paper suggests that optimization of contact angle differences between the roller and Stage 3, and the viscosity of the ink, are of extreme importance and will determine the outcome of the final printed pattern. The UV LED-curable ink had non-Newtonian dilatant, STF behavior. This UV LED-curable ink was successfully printed by use of Inkjet and 3D printing technology.

ACKNOWLEDGEMENT

The authors are grateful for the financial support from NSF Grant (EEC-1343607).

REFERENCES

1. R. Das, *Printed Electronics Europe* (Berlin: The Estrel Convention Center, 2014).
2. A. Wu, Y. Gu, C. Beck, Z. Iqbal, and J.F. Federici, *Sens. Actuators B Chem.* 193, 10 (2014).
3. D.H. Ahmed, J.S. Hyung, and D.S. Kim, *Int. J. Heat Fluid Flow* 32, 298 (2011).
4. M.K. Kwak, K.H. Shin, E.Y. Yoon, and K.Y. Suh, *J. Colloid Interface Sci.* 343, 301 (2010).
5. W.Y. Yue, C.W. Li, T. Xu, and M. Yang, *Biosens. Bioelectron.* 41, 675 (2013).
6. J.H. Hwang and K.L. Mendoza, *J. Control Sys. Eng.* 1, 67 (2013).
7. C.J. Chang, Y.H. Lin, and H.Y. Tsai, *Thin Solid Films* 519, 5243 (2011).
8. J. Perealer, P.J. Smith, D. Mager, D. Soltman, S.K. volkman, V. Subramanian, J.G. Korvinkdf, and U.S. Schubert, *J. Mater. Chem.* 20, 8446 (2010).
9. M. Pudas, J. Hagberg, and S. Leppavuori, *Prog. Org. Coat.* 49, 324 (2004).
10. S.G. Bucellaa, G. Navaa, C.K. Vishunubhatlaa, and M. Caironi, *Org. Electron.* 14, 2249 (2013).
11. M. Hui, Z. Huang, L. Cheng, and W. Shi, *Prog. Org. Coat.* 64, 365 (2009).
12. R. Sliz, Y. Suzuki, T. Fabritius, and R. Myllyla, *Colloids Surf. A* 443, 182 (2014).
13. F. Ghadiria, D.H. Ahmeda, H.J. Sunga, and E. Shirani, *Int. J. Heat Fluid Flow* 32, 308 (2011).
14. F.C. Krebs, *Sol. Energy Mater. Sol. Cells* 93, 465 (2009).
15. C. Decker, *Macromol. Rapid Commun.* 23, 1607 (2002).
16. M.M. El-Molla, *Dyes Pigments* 74, 371 (2007).
17. I.J. Zvonkina, P. Gkountara, M. Hilt, and M. Franz, *Prog. Org. Coat.* 56, 297 (2006).